# On Efficient Packet-Switched Wireless Networking: A Markovian Approach to Trans-Layer Design and Optimization of ROHC

Wenhao Wu, Student Member, IEEE, and Zhi Ding, Fellow, IEEE

Abstract—In packet-switched radio links, the little known Robust Header Compression (ROHC) has become an integral part of many wireless and particularly cellular communication networks. To strengthen existing schemes, this paper aims to improve ROHC performance in terms of payload efficiency for U-mode compression under poor wireless channel conditions. We first consider the parameter optimization of current ROHC systems, for which we propose a Markov compressor model suitable for realistic unidirectional (U-mode) ROHC. We present both the steady-state analysis and the transient behavior analysis of the ROHC. More generally, we propose a novel trans-layer ROHC design concept by exploiting lower cellular network layer status information to adaptively control header compression without dedicated feedbacks. Considering practical delay and inaccuracy when acquiring lower layer information, we develop a ROHC control framework in terms of a partially observable Markov decision process. Our results demonstrate the strength of our Markov ROHC compressor model in characterizing both stationary and transient behaviors, and the significant advantage of the proposed trans-layer ROHC design approach.

Index Terms—Packet header, compression, ROHC, Markov chain, optimization, Markov decision process.

#### I. INTRODUCTION

THE tidal wave of smartphones and high speed networks has propelled and energized numerous IP based packet services over cellular wireless networks. The fierce competition for limited resources by the rapidly growing scope of services and user population makes it imperative for network operators to improve the bandwidth efficiency not only through radio resource management at PHY/MAC layers, but also by exploiting the redundancy in protocol packets. Header compression is one such an important but less known technology that has been widely adopted in many modern communication links [1], motivated by two key observations:

 Packet payloads are often as long as, or sometimes even shorter than, the accompanied packet headers [2], [3] for many network services and applications, such as VoIP, interactive games, and media streaming.

Manuscript received August 8, 2016; revised January 25, 2017 and March 23, 2017; accepted April 7, 2017. Date of publication April 24, 2017; date of current version July 10, 2017. This work was supported by the National Science Foundation under Grant CIF-1321143, Grant CNS-1443870, and Grant CNS-1702752. The associate editor coordinating the review of this paper and approving it for publication was T. Melodia. (Corresponding author: Wenhao Wu.)

The authors are with the Department of Electrical and Computer Engineering, University of California at Davis, Davis, CA 95616 USA (e-mail: wnhwu@ucdavis.edu; zding@ucdavis.edu).

Color versions of one or more of the figures in this paper are available online at http://ieeexplore.ieee.org.

Digital Object Identifier 10.1109/TWC.2017.2694840

 Packet headers are mostly compressible, as many fields in the headers remain unchanged or changes in a predictable manner in a traffic flow over a connected link.

RObust Header Compression (ROHC) has been standardized [4]-[6] to address the header compression in wireless links, characterized by high packet error rate (PER) and long round-trip time (RTT) [2] and thus conventional header compression techniques designed for wireline links are not well suited. Although the boiler-plate ROHC has found its application in a wide range of wireless packet networks [7]-[11], its analysis and optimization have only received modest research attention. Most studies [12]-[20] present simulation results on the performance of ROHC under realistic but very specific system settings, yet there exist very few attempts to comprehensively analyze ROHC performances, much less to optimize ROCH or key ROHC design parameters. Most of these analytical works about ROHC model the channel and/or packet source as random processes interacting with the ROHC compressor and the decompressor. Different performance measurements such as compression efficiency, robustness, transparency, probability of Out-of-Synchronization (OoS), the average number of bits to compress RTP sequence number, etc., are evaluated and/or optimized versus various design parameters such as encoding codebook, window width of the window-based least significant bits (WLSB) encoding algorithm, context refresh period, channel and packet source characteristics, and so forth [21]-[25]. Simplified analytical ROHC model with fixed compressor's state transition over finite ROHC session without considering header encoding is also studied in [26].

Despite of the efforts of these works to balance accuracy versus simplicity in modeling ROHC systems, many questions still remain unanswered within the existing ROHC framework. Firstly, it remains mostly unclear how to optimally select some key parameters of the unidirectional (U-mode) ROHC compressor, e.g. a set of timeout limits [4, Sec. 5.3.1.1.2.], [27, Sec. 3.3.2]. Secondly, even though ROHC was developed for wireless packet-switch links, existing ROHC designs do not make full use of the protocol infrastructure of wireless communication systems. In most designs, the ROHC resides in the upper Packet Data Convergence Protocol (PDCP) layer with little or no knowledge from lower or higher layers [7]. For instance, even without dedicated ROHC feedback channel, U-mode ROHC compressor can still deduce whether or not packets have been transmitted successfully based on information available from lower layers such as HARQ feedback [28].

Also, from lower layer information such as Channel Quality Indicator (CQI), it is possible for the ROHC compressor to estimate the previous channel states. For a timely-correlated ROHC channel as in [21] and [24], this estimation allows the compressor to predict the future channel states so as to adjust the compression level accordingly. Without a translayer design for the ROHC compressor, it remains questionable whether the full potential of ROHC has been fully realized under the existing "stand-alone" design philosophy.

Among the contributions of this paper, we first propose a U-mode ROHC parameter optimization scheme based on the Markovian approximation of a timer-based ROHC compressor. The performance is examined in a finite-state Markov channel model much more general and practical than the Gilbert-Elliot model used in [24] and [28]. The design objective is to maximize the transmission efficiency of the ROHC link. The "slow-start" mechanism is also incorporated to characterize the transient ROHC behavior. These results lead to an integrated Markov model for the entire ROHC system consisting of the compressor, the channel, and the decompressor, where the Markovian approximation of the compressor greatly reduces the state space than the timer-based ROHC compressor. Secondly, to fully explore the potential of ROHC, we propose a novel trans-layer ROHC compressor design to utilize lower layer information to dynamically adjust the compression level. Unlike in [28], our practical consideration takes into account of the imperfect and delayed estimation on the transmission status and channel states, leading to a new dynamic control framework in the form of partially observable Markov decision process (POMDP), a decision-making tool with successful applications in many fields [29], [30] and wireless communications in particular recently [31]-[40]. Different from [41], our proposed POMDP-based ROHC framework adopts a true trans-layer design by exploring lower layer signaling without introducing additional feedback mechanism on the ROHC layer. Also, our design focuses on adapting ROHC to lower layer channel conditions, instead of adjusting lower layer forward error correction (FEC) mechanism to ROHC studied in [42]. Our results demonstrate how the performance of ROHC system is impacted by the design parameters of the Markov model for optimization, as well as the advantages of the trans-layer design methodology.

We organize the manuscript as follows. Section II describes the key components of the ROHC system in simple terms and specifies the channel model used in this work. Section III delineates the analytical U-mode ROHC compressor model and the Bayesian representation of the integrated Markov model for the entire ROHC system including the compressor, the channel, and the decompressor. Section IV depicts the POMDP formulation of our trans-layer ROHC compressor design. We present a general POMDP solution as well as a detailed complexity analysis in Section V. Section VI delivers numerical results before Section VII concludes the work.

#### II. SYSTEM MODEL

## A. Notations

The following notational conventions are used throughout this paper. Scalars, vectors, matrices and sets are represented

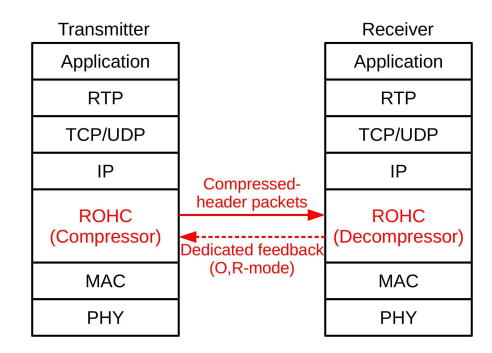


Fig. 1. Wireless ROHC header compressor and decompressor in the protocol stack of a packet switched network.

with regular font, bold-face lower-case, bold-face uppercase, and calligraphic letters, respectively. Matrix transpose is denoted with  $(\cdot)^T$ . The Cartesian product of sets  $\mathcal{A}$  and  $\mathcal{B}$ is denoted as  $\mathcal{A} \times \mathcal{B}$ . All the Markov matrices are written as left stochastic matrix in which each column sums to 1, and all the probability vectors are column vectors. As a naming rule throughout this manuscript, the subscript "C", "H", "D" and "T" stands for "compressor", "channel" and "decompressor" and "transmission", respectively. And in the Markov model, state variables with and without prime symbol (e.g. s' and s) represent the next state and the current state, respectively. The time index, i.e. the sequence number of the n-th packet/timeslot, is denoted as "[n]". We use C language style notation for indexing variables which starts from 0.

### B. An Introduction to ROHC System

Fig. 1 depicts the location and functionality of ROHC header compressor and decompressor in the protocol stack of a packet-switched wireless network. In a typical ROHC mechanism, each packet stream must rely on its own compressor and decompressor. We focus on a simple model in which a U-mode ROHC compressor transmits a packet stream with compressed headers whereas a corresponding remote decompressor receives and recovers the packet header (along with the full packet recovery by the receiver). This work focuses on the compressor design for unidirectional (U-mode) ROHC in which there is no ROHC feedback, unlike bidirectional optimistic (O-mode) and reliable (R-mode) ROHC in which available feedback greatly simplifies the state transition logic of the compressor. U-mode ROHC is important since ROHC must always start from the U-mode before transitioning into other modes (if so designed) [4, Sec. 4.4.1].

As described in [4, Secs. 4.3.1 and 5.3.1], the U-mode compressor can be modeled as a finite-state machine (FSM) with three states, each represented with the type of packets transmitted at this state. The fields of a packet header can be roughly categorized as being static, which does not change throughout the packet session (e.g. IP address), and dynamic, which changes regularly and mostly in specific patterns and thus can be compressed, for example, with a non-constant serial number (e.g. IP ID) [2]. The compressor always starts in the Initialization and Refresh (IR) state by transmitting IR packets, whose headers are not compressed, to establish

context synchronization. First-Order (FO) packets are usually partially compressed, which contain differential information of the dynamic fields and rarely a few static fields, in order to efficiently communicate irregularities in the packet stream. Finally, the header of the Second-Order (SO) packets are fully compressed. The compressor state transitions upwards to higher order states (FO and SO) by sending several packets within each lower state (i.e., IR and FO) to gain enough confidence with respect to context synchronization by the remote decompressor without receiving decompressor feedback. It also needs to transition downward based on timeouts and the need for updates [27, Sec 3.3] to prevent the context at the compressor and the decompressor to become outof-synchronization (OoS) due to loss of packets. Since we focus on the compressor optimization against lossy channel, we assume that the input to the compressor is always regular/compressible, such that downward transition to FO state is only needed to recover context synchronization and downward transition to IR state is not necessary. For modeling of the packet source we refer our readers to [24].

Correspondingly, the decompressor is also modeled as a FSM with three states [4, Secs. 4.3.2 and 5.3.2]. In the Non-Context (NC) state, the decompressor requires initialization and can only decode IR packets. Upon successful reception of at least one IR packet, thereby establishing context for both the static and dynamic field, the decompressor transitions upward to the Full-Context (FC) state, in which all three types of (IR, FO, SO) packets can be decoded. In case of repeated decompression failures, the decompressor could also transition back down to an intermediate Static-Context (SC) state, where one FO or IR packet would suffice to re-establish context synchronization to move the decompressor upwards again to FC state. In this work, we have assumed that the packet source is always compressible and a decompression failure is solely caused by transmission error. Consequently, a single FO packet transmitted successfully is sufficient for upward transition from SC to FC, and for the original "k-outof-n" downward transition rule we can set k = n = 1. Despite being derived from our regular packet source assumption, both conditions are highly realistic [4, Secs. 4.3.2 and 5.3.2.2.3].

A key header compression technique is the Window-based Least Significant Bits (WLSB) algorithm which is adopted on many header fields [4, Sec. 4.5.2]. As a modification of the Least Significant Bits algorithm, the WLSB compressor maintains a reference window based on which the compressor decides to transmit k LSBs. Upon receiving the compressed header verified by CRC, the decompressor is able to figure out the complete header by identifying the only possible value in the interpretation interval, as long as the its reference value resides in the compressor's window. In this work, we characterize the robustness of our ROHC system based on WLSB encoding with a single parameter W, i.e., the maximum number of packets that can be lost consecutively without losing context synchronization [21]. We note that the selection of the WLSB parameters is out of the scope of our work here and readers may review [23] for more details. Combined with the aforementioned FSM-model, our decompressor model is similar to model 2 in [21].

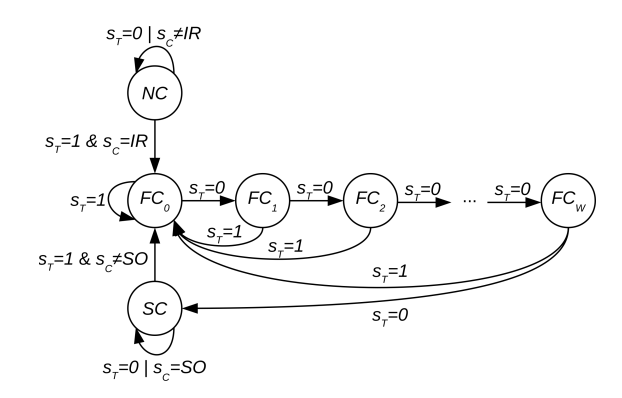


Fig. 2. Finite state machine (FSM) model of the ROHC decompressor, whose state transition depends on the transmission status of the channel  $(s_T)$  and the header type from the compressor  $(s_C)$ .

In summary, the work flow of our ROHC model during a packet session is demonstrated with the state transition diagram of the decompressor dependent on the transmission status and the header type from the compressor as shown in Fig. 2. The state of the decompressor is represented by  $s_D = FC_0, ..., FC_W, SC, NC$ , where  $FC_w$  denotes the decompressor still maintaining full context but a consecutive of w packets have been lost. Also,  $s_T = 1$  and  $s_T = 0$ represent successful/failed transmission of a packet and s<sub>C</sub> denotes the header type. Initially, the decompressor always starts from the NC state. Upon the successful transmission of an IR packet with a full header, both the static and the dynamic context have been established and thus the decompressor enters the FC<sub>0</sub> state and is able to decompress all three types of packets if transmitted successfully. As long as the decompressor maintains full context ( $s_D = FC_0, ..., FC_W$ ), the successful transmission of any type of packet will lead the decompressor back to FC<sub>0</sub> state. If a consecutive of W + 1transmission has failed, the dynamic context will be lost and the decompressor enters the SC state where it is only able to decompress IR or FO packet. Upon the successful transmission of either of these two types of packets, the decompressor will transition back to FC<sub>0</sub> state. For notational convenience, we denote  $s_D = w$ , w = 0, ..., W as the decompressor being in  $FC_w$  state, while  $s_D = W + 1$  and  $s_D = W + 2$  as SC and NC state, respectively. In the following section we also denote  $s_C = 0, 1, 2$  as IR, FO and SO headers, respectively.

#### C. Channel Model

Existing work [24] on ROHC adopts the Gilbert-Elliot model [43] for the time-varying ROHC channel. However, in practice the channel quality may not be so clear-cut into only two states. It is even less likely that the transmission in "good" state always succeeds and that in the "bad" states always fails as assumed in [21]. Due to error-control measures in lower layer of the protocol stack such as link-adaptation and HARQ, it would be more reasonable to characterize the ROHC channel into more than two states, each associated with a known probability of successful transmission, as suggested in the original Gilbert-Elliott model [44]. Moreover, since different ROHC headers generate different packet lengths

to be segmented/aggregated at lower layers, in general the channel for different types of packets needs to be characterized individually.

In this work, we consider a general finite-state Markov channel (FSMC) [45], [46] with K states, whose parameters can be estimated from wireless traces with, for example, a modified Baum-Welch algorithm [47]. The transition matrices of this channel are denoted by a K-by-K matrix  $\mathbf{P}_H$  and the probability of successful transmission of IR, FO and SO packets are denoted by  $\rho_{SC}$ ,  $S_C = 0, 1, 2$  respectively.

### D. Assumptions

To enable a simple yet meaningful analysis, we make the following practical assumptions on our system model:

- A1 The three types of headers and the payload capsules in a packet have fixed lengths, denoted as  $H_0$ ,  $H_1$ ,  $H_2$  and  $L_P$ , respectively, such that  $H_0 > H_1 > H_2$  would reflect different compression levels of IR, FO and SO headers. The total length of IR, FO and SO packets are denoted as  $L_0$ ,  $L_1$ ,  $L_2$ , respectively, where  $L_i = H_i + L_P$ , i = 0, 1, 2.
- A2 We let  $\rho_0 \leq \rho_1 \leq \rho_2$  to represent the probability of successful transmission of IR, FO and SO packets, respectively, where  $\leq$  denotes entry-wise less than or equal to relationship.
- A3 As shown in Fig. 2, as long as one IR packet is transmitted successfully, the decompressor is never going back to the NC state.

Assumption A1 is meant to facilitate a straightforward analysis. In reality, there are more than one types of FO (e.g. IR-DYN, UOR-2, etc.) and SO packets (e.g. UO-0, UP-1, etc.) and the payload length may also vary. Such subtle differences can be neglected. Assumption A2 suggests that under the same channel condition, longer packets are more prone to packet loss. Assumption A3 is due to the fact that the static fields of the headers remain unchanged throughout the entire lifespan of the packet stream [4, Sec. A.1]. Consequently, we expect an efficient design of ROHC compressor to transmit many IR packets at the beginning of the packet session and before alternatingly transmit the shorter FO and SO packets. This design philosophy can be deliberately enforced by "slow-start" in conventional ROHC compressor (Section III-D). On the other hand, our proposed trans-layer ROHC compressor is able to decide when to transmit IR packets based on belief on the decompressor's states updated with lower layer channel information (Section IV-B).

# III. OPTIMIZATION OF CONVENTIONAL U-MODE ROHC COMPRESSOR

The state transition for a U-mode ROHC compressor is determined by several timer/counters [4, Sec. 5.3.1.1], which leads to deterministic, periodic behavior easy to implement. However, in terms of performance analysis and optimization, this model is undesirable in that it is difficult to derive a relationship between the average performance measurement and the parameters without Monte-Carlo simulation. A rigorous Markov modeling of the ROHC system with the periodic

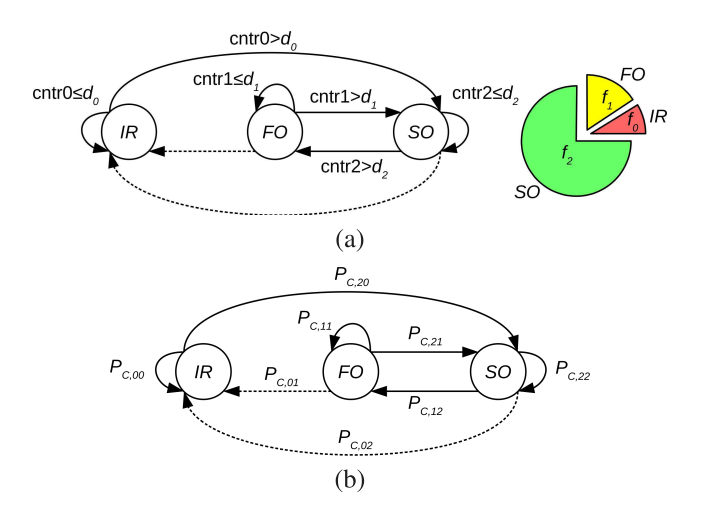


Fig. 3. (a) The timer-based U-mode ROHC compressor model characterized by  $f_0$ ,  $f_1$ ,  $f_2$  and  $d_0$ ,  $d_1$ ,  $d_2$ . "cntr" stands for "counter". (b) The corresponding Markov ROHC compressor model characterized by  $\mathbf{P}_C$ .

compressor would result in a prohibitively large state space if the period is large.

To overcome this dilemma of the timer-based U-mode ROHC compressor, we approximately model it as a Markov process that is much more amenable to theoretical analysis and optimization. We identify a few key characterizing variables which can be evaluated for both conventional ROHC compressor and the Markov ROHC compressor, and derive a one-to-one mapping between the design parameters of the two models. Consequently, to analyze a timeout based ROHC compressor, we first map it onto a Markov ROHC compressor; we then carry out the analysis/optimization on the Markov ROHC compressor before mapping the results back to the timeout based ROHC compressor.

#### A. Markov Chain Modeling of Practical Compressor

The Markov compressor has the same three states as the conventional ROHC compressor, characterized by a 3-by-3 state transition matrix  $\mathbf{P}_C$ . The entry  $P_{C,ij}$  is the probability of transition from state j to state i, where i, j = 0, 1, 2 denotes IR, FO and SO, respectively.

The stationary behavior of any U-mode compressor can be approximately characterized by 6 design parameters, namely  $f_{s_C}$  and  $d_{s_C}$ , which represents the fraction and the average duration of consecutive transmission of IR, FO and SO packets, respectively, where  $s_C = 0$ , 1, 2 denote IR, FO, and SO packets, respectively (Fig. 3). Because of the constraint  $\sum_{s_C=0}^{2} f_{s_C} = 1$ , these 6 parameters actually have a degreeof-freedom (DOF) equal to 5. In comparison,  $P_C$  has a DOF equal to 6. To facilitate a 1-to-1 mapping between the two set of parameters, we note that in practice it makes no sense for the compressor to transition from IR state to FO state, instead of directly transitioning to SO state. Consequently, we let  $P_{C,10} = 0$ . For the Markov compressor,  $\mathbf{f} = [f_0, f_1, f_2]^T$ denotes simply the steady-state distribution of  $P_C$ , whereas  $d_0$ ,  $d_1$ ,  $d_2$  denote the mean durations of the three states, respectively. In summary, the two set of parameters can be

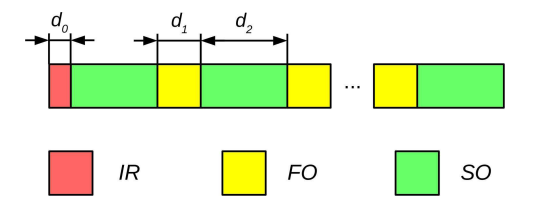


Fig. 4. Periodic operation of U-mode compressor based on timeout.

mapped from one to the other by solving

$$d_0 = \frac{1}{P_{C,20}}, \ d_1 = \frac{1}{P_{C,01} + P_{C,21}}, d_2 = \frac{1}{P_{C,02} + P_{C,12}},$$
$$\mathbf{P}_C \mathbf{f} = \mathbf{f}. \tag{1}$$

and such mapping has the feasibility region:

$$\mathcal{F} = \left\{ (f_0, f_1, f_2, d_0, d_1, d_2) : \frac{f_2}{d_2} \ge \frac{f_1}{d_1}, \frac{f_2}{d_2} \ge \frac{f_0}{d_0}, \\ \frac{f_0}{d_0} + \frac{f_1}{d_1} \ge \frac{f_2}{d_2}, d_{s_C} \ge 1, s_C = 0, 1, 2. \right\}.$$
 (2)

It is easy to verify that a typical timer-based U-mode ROHC compressor [26, Fig. 5] which transmits one segment IR packet and *N* segments of FO and SO packets alternatingly within each period, as shown in Fig. 4, satisfies the feasibility conditions. Instead of optimizing the timeout-based ROHC compressor directly, we optimize the parameters of the approximated Markov compressor, and then map its parameters back to that of the timeout-based ROHC compressor. Our simulation results in Section VI demonstrates the effectiveness of this approach. Next we focus on the performance evaluation and optimization of the approximated Markov compressor.

### B. Performance Metrics and Optimization

By modeling the U-mode ROHC compressor as a Markov process, the entire ROHC system consisting of the compressor, the channel and the decompressor can now be formulated as one integrated Markov process. To see this, we denote the system state as a 3-tuple  $\mathbf{s} = (s_C, s_D, s_H) \in \mathcal{S}$ , where  $s_C \in S_C = \{0, 1, 2\}, s_D \in S_D = \{0, \dots, W + 2\}$  and  $s_H \in S_H = \{0, \dots, K-1\}$  are the compressor's state (header type of the next packet), the decompressor's state and the channel's state (last realization), respectively. The ROHC system's state space  $S = S_C \times S_D \times S_H$  has a cardinality of 3(W+3)K. As explained in Sec. II-C, the transmission status  $s_T$  depends on  $s_C$  and  $s'_H$ . The state transition probability is illustrated as a dynamic Bayesian network (DBN) [48, Sec. 8.2] in Fig. 5, where circles represent random variables (RV) and arrows represent conditional dependency. The transition probability of the overall Markov model is

$$p(\mathbf{s}'|\mathbf{s}) = p(s_C'|s_C)p(s_H'|s_H)p(s_D'|s_D, s_C, s_H')$$
(3)

where  $p(s'_C|s_C)$  and  $p(s'_H|s_H)$  are defined by  $\mathbf{P}_C$  and  $\mathbf{P}_H$ , respectively, and

$$p(s'_{D}|s_{D}, s_{C}, s'_{H}) = p(s'_{D}|s_{D}, s_{T} = 1, s_{C})p(s_{T} = 1|s_{C}, s'_{H}) + p(s'_{D}|s_{D}, s_{T} = 0, s_{C})p(s_{T} = 0|s_{C}, s'_{H})$$
(4)

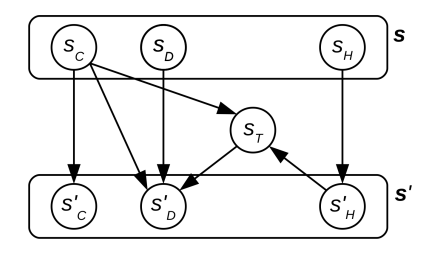


Fig. 5. Dynamic Bayesian network (DBN) representation of the ROHC system with the Markov compressor.

where  $p(s_T = 1|s_C, s_H') = \rho_{s_C, s_H'}$  and  $p(s_D'|s_D, s_T, s_C) \in \{0, 1\}$  are defined by Fig. 2.

The primary benefit for formulating such an integrated Markov model is that many performance metrics can be readily defined using its (marginal) stationary distribution. For instance, we can define the compression transparency  $\tau$  as the probability that the decompression is successful, conditioned on a successful transmission. We note that a decompression success is equivalent to the event of  $s_D' = 0$ . Thus,

$$\tau = p(s_D' = 0 | s_T = 1) = 1 - \frac{p(s_D' \neq 0, s_T = 1)}{p(s_T = 1)}$$
 (5)

in which

$$p(s'_{D} \neq 0, s_{T} = 1) = \sum_{s_{H}=0}^{K-1} \sum_{s'_{H}=0}^{K-1} p(s_{C} = 2, s_{D} = W + 1, s_{H})$$

$$\times p(s'_{H}|s_{H}) p(s_{T} = 1|s_{C} = 2, s'_{H}) \quad (6)$$

$$p(s_{T} = 1) = \sum_{s_{C}=0}^{2} \sum_{s'_{H}=0}^{K-1} \pi_{C,s_{C}} \pi_{H,s'_{H}} p(s_{T} = 1|s_{C}, s'_{H})$$

$$(7)$$

where  $p(s_C = 2, s_D = W + 1, s_H)$  is the full stationary probability for state  $\mathbf{s} = (2, W + 1, s_H)$ , whereas  $\pi_{C,s_C}$  and  $\pi_{H,s_H'}$  represent the marginal stationary probability of the compressor being in state  $s_C$  and that of the channel being state  $s_H'$ , respectively.  $\tau$  serves as an indicator of how well the ROHC avoids unnecessary packet loss caused by header compression. Against such packet losses, upper layers may have to retransmit, causing extra delays.

In this work, we consider compressor optimization to maximize the transmission efficiency  $\eta$ , which directly measures the effective bandwidth usage of a packet-switched link equipped with ROHC. Specifically, define  $\eta$  as the ratio of the expected number of decompressed payload bytes to that of the transmitted bytes (including header and payload), namely

$$\eta(\mathbf{P}_C) = \frac{\pi_{D,0} L_P}{\sum_{s_C=0}^2 \pi_{C,s_C} L_{s_C}}$$
(8)

where  $\pi_{D,0}$  stands for the marginal stationary probability of the decompressor for  $s_D = 0$ .

Because it is difficult, if not impossible, to derive a closed form for the stationary distribution of the ROHC system, our approach solves the problem numerically. At first glance, there are 5 variables in  $\mathbf{P}_C$  to optimize, which represents a very large search space. In order to simplify the compressor

design problem, we note that, as mentioned in Section II-D, it is desirable for a ROHC compressor to transmit only FO and SO packets alternatingly after the establishment of context synchronization. This is because FO packets have less header overhead and are less vulnerable to packet loss than IR packets. Thus,  $\pi_{C,0}=0$ . However, its optimality is not guaranteed as  $\mathbf{P}_C$  may not exhibit such property in general. Also, since the decompressor always starts in the NC state, it must receive enough IR packets to establish context synchronization.

In the following, we will first show that under certain conditions our Markov compressor model indeed favors transmitting only FO and SO packets. We then show how protocol-dictated "slow-start" action can be integrated into our Markov ROHC compressor to ensure context synchronization by transmitting more IR packets during the initial phase of a ROHC session.

# C. Conditions for the Simplification of $P_C$

From Fig. 2, since  $s_T=1$  is a necessary condition for  $s_D'=0$ , we have  $\pi_{D,0}=p(s_D'=0,s_T=1)$ . Hence (8) can be rewritten as

$$\eta(\mathbf{P}_C) = \frac{L_P p(s_T = 1)\tau}{\sum_{s_C = 0}^2 \pi_{C, s_C} L_{s_C}}.$$
 (9)

We note that both  $p(s_T = 1)$  and the denominator in (9) depend on the Markov compressor only via its stationary distribution. We construct the following surrogate compressor

$$\bar{\mathbf{P}}_C = \begin{bmatrix} 0 & 0 & 0 \\ 0 & \bar{P}_{C,11} & P_{C,02} + P_{C,12} \\ 1 & \bar{P}_{C,21} & P_{C,22} \end{bmatrix}$$
(10)

where

$$\bar{P}_{C,21} = \frac{P_{C,20}\pi_{C,0} + P_{C,21}\pi_{C,1}}{\pi_{C,0} + \pi_{C,1}}, \quad \bar{P}_{C,11} = 1 - \bar{P}_{C,21} \quad (11)$$

which is directly related to the quotient Markov chain [49]. The stationary probability of  $\bar{\mathbf{P}}_C$  is coherent with that of  $\mathbf{P}_C$ , i.e.  $\bar{\pi}_{C,0} = 0$ ,  $\bar{\pi}_{C,1} = \pi_{C,0} + \pi_{C,1}$  and  $\bar{\pi}_{C,2} = \pi_{C,2}$ .

Since  $H_1 > H_0$  whereby  $L_1 > L_0$ , the denominator in (9) of  $\eta(\bar{\mathbf{P}}_C)$  is no larger than that of  $\eta(\mathbf{P}_C)$ . As long as  $\tau(\mathbf{P}_C) \approx \tau(\bar{\mathbf{P}}_C)$ , which is verified numerically in Section VI,  $\bar{\mathbf{P}}_C$  tends to generate larger efficiency  $\eta$ . Consequently, in order to maximize the transmission efficiency  $\eta$  over  $\mathbf{P}_C$ , we can fix  $P_{C,01} = P_{C,02} = 0$  such that eventually only FO and SO packets are transmitted alternatingly. This is in accordance with the fact that, in practice, when the decompressor is in the SC state, reception of any packet sent in the FO state is normally sufficient to enable transition to resume context synchronization [4, Sec. 4.3.2]. As a result, we have  $\bar{\pi}_{C,0} = 0$  since the corresponding states are transient. Now the maximization of  $\eta$  is reduced to an optimization problem with respect to  $P_{C,11}$  and  $P_{C,22}$  only, instead of  $\mathbf{P}_C$  which has 5 independent variables in the search space.

Under this condition, we can study a reduced Markov compressor with only two states  $s_C = 1, 2$ . Correspondingly, the Markov transition matrix for the ROHC system with reduced state space  $S_R = \{\mathbf{s} | \mathbf{s} \in S, s_C \neq 0\}$  is defined as

$$\mathbf{P}_{S} = \begin{bmatrix} P_{C,11}\mathbf{T}_{1} & (1 - P_{C,22})\mathbf{T}_{2} \\ (1 - P_{C,11})\mathbf{T}_{1} & P_{C,22}\mathbf{T}_{2} \end{bmatrix}$$
(12)

where

$$\mathbf{T}_{1} = \begin{bmatrix} \mathbf{A}_{1} & \cdots & \mathbf{A}_{1} & \mathbf{A}_{1} & \mathbf{0} \\ \mathbf{B}_{1} & & \mathbf{0} & \mathbf{0} & \mathbf{0} \\ \mathbf{0} & \ddots & \vdots & \vdots & \vdots \\ \vdots & & \mathbf{B}_{1} & \mathbf{B}_{1} & \mathbf{0} \\ \mathbf{0} & \cdots & \mathbf{0} & \mathbf{0} & \mathbf{P}_{H} \end{bmatrix},$$

$$\mathbf{T}_{2} = \begin{bmatrix} \mathbf{A}_{2} & \cdots & \mathbf{A}_{2} & \mathbf{0} & \mathbf{0} \\ \mathbf{B}_{2} & & \mathbf{0} & \mathbf{0} & \mathbf{0} \\ \mathbf{0} & \ddots & \vdots & \vdots & \vdots \\ \vdots & & \mathbf{B}_{2} & \mathbf{P}_{H} & \mathbf{0} \\ \mathbf{0} & \cdots & \mathbf{0} & \mathbf{0} & \mathbf{P}_{H} \end{bmatrix}$$

$$(13)$$

where  $\mathbf{A}_{s_C} = \operatorname{diag}(\boldsymbol{\rho}_{s_C})\mathbf{P}_H$  and  $\mathbf{B}_{s_C} = \mathbf{P}_H - \mathbf{A}_{s_C}$ ,  $s_C = 1, 2$ . Note that, however,  $\mathbf{P}_S$  has two closed communication classes, i.e.  $S_1 = \{\mathbf{s}|s_D \neq W+2, s \in S_R\}$  and  $S_2 = S_R \setminus S_1$ . Therefore, its stationary distribution is not uniquely defined. To tackle this issue, it is ensured by the slow-start operation to be introduced next that enough IR packets have been transmitted before the compressor enters the stationary distribution such that the decompressor is not in NC state. Consequently, the stationary distribution of the ROHC system can be uniquely defined with non-zero values over  $S_1$ .

In summary, the optimization of the Markov compressor is well-defined as

$$\max_{P_{C,11}, P_{C,22}} \eta$$
, s.t.  $0 \le P_{C,11} \le 1$ ,  $0 \le P_{C,22} \le 1$  (14)

which can be easily solved with general-purpose optimization tools or a basic 2-D grid search.

#### D. The Slow-Start Strategy

The maximization of efficiency  $\eta$  in (14) is based on the steady-state analysis of our Markov model. However, in practice, when a ROHC session starts, the initial state of the system must have  $s_C = 0$  and  $s_D = W + 2$ . As a result, when directly applying the optimized Markov compressor, there shall only be a limited number of IR packets transmitted on average before the compressor transitions into other states and would not transmit IR packets again. Consequently, the decompressor has a non-negligible chance of never leaving the NC state. Thus, the ROHC system may not converge to the desired stationary distribution corresponding to max  $\eta$ .

This scenario directly justifies the strategy of transmitting IR packets more frequently in the beginning of a ROHC session. One such strategy already adopted in practical ROHC compressor is called slow-start [4, Sec. 5.3.1.1.2], [27, Sec. 3.3.1], in which an uncompressed IR packet is transmitted with exponentially increasing intervals. To imitate this operation so as to actually approach the maximum  $\eta$ , we define the following time-varying Markov compressor based on the optimal  $\hat{\mathbf{P}}_C$  from the previous section:

$$\hat{\mathbf{P}}_C[n] = \begin{cases} \mathbf{P}_{C,0} & 1 \le n \le n_{max} \text{ and } n = i - 2 + 2^i \\ \hat{\mathbf{P}}_C & \text{otherwise} \end{cases}$$
 (15)

where n=0,1,... is the index of the transmitted packet,  $n_{max}$  is the duration of the slow-start phase and

 $\mathbf{P}_{C,0} = [0, 1, 1; 0, 0, 0; 1, 0, 0]$ . The optimal  $\hat{\mathbf{P}}_C$  has  $\hat{P}_{C,11}$  and  $\hat{P}_{C,22}$  optimized as in the previous section and  $\hat{P}_{C,00} = 0$  is in accordance with [27] in which only one full header is sent each time. The Markov compressor defined by (15) strictly ensures that when  $n < n_{max}$  there is one IR packet transmitted with growing intervals as a power of 2. If the slow start-phase is long enough therefore enough IR packets has been transmitted, then asymptotically the compressor can be reduced to have only two states (FO and SO). As long as  $\hat{P}_{C,11} \neq 0$  or  $\hat{P}_{C,22} \neq 0$  and  $\mathbf{P}_H$  is ergodic, it is easy to verify that  $\mathbf{P}_S$  is also ergodic and thus the stationary distribution is uniquely defined. In practice,  $n_{max}$  can be selected based on numerical simulations, but it is inherently impossible to achieve the optimal performance in both the transient and the stationary stage, as to be shown in Section VI.

# IV. A New Trans-Layer U-Mode ROHC COMPRESSOR DESIGN

Thus far, we have focused on optimizing the conventional U-mode ROHC compressor based on statistical information regarding the ROHC channel. To further improve the efficiency and reliability of ROHC U-mode without requiring explicit and costly feedback channel as in O-mode and R-mode, we now present a new trans-layer framework for controlling ROHC compressor by leveraging useful information obtained from the lower layers to obtain partial information of the decompressor's state.

#### A. Exploiting Trans-Layer Information

We note at least two types of lower layer information available for ROHC control at the PDCP layer:

- 1) A status estimate of whether or not the previous ROHC packets have been transmitted successfully. This estimate can benefit, for example, from the HARQ feedback as discussed in [28]. It is characterized by the false alarm probability  $P_{\rm FA}$  and the mis-detection probability  $P_{\rm MD}$  for the detection of transmission failures.
- 2) An estimate of the previous ROHC channel state. This information can be acquired by analyzing the control signaling from lower-layers (e.g., CQI reports from PHY, link-adaptation, etc.). The channel estimator's performance is characterized by matrix  $\mathbf{E}_H$ , whose entry  $E_{H,ij}$  is the probability that the estimated channel state in i when the true channel state is j.

Ideally, it is possible to get the transmission status estimation and channel state estimation for the most recent ROHC packet. However, in practice, due to the transmission and processing delay of, for example, the HARQ and CQI feedbacks, the ROHC compressor at the transmitter's PDCP layer may only acquire lower layer information with d ROHC packet delay. We will address this problem by extending the state space after formulating a basic trans-layer ROHC compressor without observation delays.

#### B. A POMDP Formulation

For ROHC context synchronization, it is important for the compressor to process packet headers in accordance with the

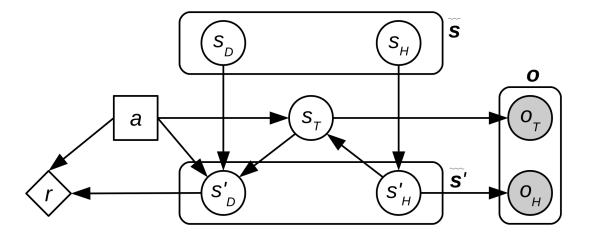


Fig. 6. DBN representation of the ROHC system with the trans-layer POMDP compressor.

decompressor's state. However, the compressor does not have a direct knowledge on the U-mode decompressor's state. Our POMDP formulation aims to allow the compressor, without a direct state feedback from the decompressor, to estimate the state of a U-mode decompressor based on partial observations from lower layer signaling.

Our fundamental principle is that, based on the initial state of the decompressor, the transmission and channel state estimation, a belief on the ROHC system's state can be continuously updated, and an optimal decision can be made regarding the type of packet header to transmit next. This problem can be formulated into a partially-observable Markov decision process (POMDP) [50]. First, we consider the simple case of zero-delay estimation where d=0, represented as a DBN in Fig. 6. Our trans-layer ROHC compressor is formulated into a POMDP defined by the following elements [50, Definition 12.2.1]:

- State of the system: Defined as the Cartesian product of the decompressor's state and the channel's state  $\tilde{\mathbf{s}} = (s_D, s_H) \in \tilde{\mathcal{S}} = \mathcal{S}_D \times \mathcal{S}_H$ .
- Action of the agent: The POMDP compressor decides the type of packets to transmit next, which is defined as  $a \in \mathcal{A} = \mathcal{S}_C = \{0, 1, 2\}.$
- Observation: Defined as the combination of packet status estimation and channel estimation  $\mathbf{o} = (o_T, o_H) \in \Omega = \Omega_T \times \Omega_H$  where  $o_T \in \Omega_T = \{0, 1\}$  has the same meaning as  $s_T$ , and  $\Omega_H = S_H = \{0, \dots, K-1\}$ .  $\Omega_T$  and  $\Omega_H$  represent the observation space of the transmission status and the channel state, respectively.
- Probabilistic transition function  $T(\tilde{\mathbf{s}}, a, \tilde{\mathbf{s}}') = p(\tilde{\mathbf{s}}'|\tilde{\mathbf{s}}, a)$ : the probability of transition from  $\tilde{\mathbf{s}}$  to  $\tilde{\mathbf{s}}'$  given action a. This function is defined as

$$T(\tilde{\mathbf{s}}, a, \tilde{\mathbf{s}}') = p(s_H'|s_H)p(s_D'|s_D, a, s_H')$$
 (16)

in which  $p(s'_D|s_D, a, s'_H)$  is defined exactly the same as (4) by replacing  $s_C$  with a.

• Observation function  $O(\tilde{\mathbf{s}}', a, \mathbf{o}) = p(\mathbf{o}|\tilde{\mathbf{s}}', a)$ : the probability of observing  $\mathbf{o}$  in state  $\mathbf{s}'$  after executing a. This function can be defined as

$$O(\tilde{\mathbf{s}}', a, \mathbf{o}) = p(o_H | s_H') p(o_T | a, s_D', s_H')$$
 (17)

where  $p(o_H|s'_H)$  is defined by the channel estimation matrix  $\mathbf{E}_H$  whereas

$$p(o_T|a, s'_D, s'_H) = p(o_T|s_T = 1)p(s_T = 1|a, s'_D, s'_H) + p(o_T|s_T = 0)p(s_T = 0|a, s'_D, s'_H).$$
(18)

Here  $p(o_T|s_T)$  is defined by  $P_{FA}$  and  $P_{MD}$ . Moreover,  $p(s_T|a, s_D', s_H')$  can be evaluated as:

- If  $s'_D = 0$ , the transmission must have been successful, i.e.,  $p(s_T = 1|a, s'_D, s'_H) = 1$ .
- If  $s'_D = 1, ..., W$ , the transmission must have failed, i.e.  $p(s_T = 1 | a, s'_D, s'_H) = 0$ .
- If  $s'_D = W + 1$ , when a = 0, 1,  $p(s_T = 1|a, s'_D, s'_H) = 0$ ; When a = 2, there is no knowledge on whether the transmission was successful or not without knowing  $s_D$ . Hence, the best action one can do is to "infer" the transmission status according to the channel state, i.e.  $p(s_T = 1|a, s'_D, s'_H) = p(s_T = 1|a, s'_H) = \rho_{a, s'_H}, a \in \mathcal{A}$ .
- Similarly, if  $s'_D = W + 2$ , then for a = 0, we have  $p(s_T = 1 | a, s'_D, s'_H) = 0$ ; For a = 1, 2,  $p(s_T = 1 | a, s'_D, s'_H) = p(s_T = 1 | a, s'_H) = \rho_{a, s'_H}$ .
- Reward function  $R(\tilde{s}, a, \tilde{s}')$ , the immediate reward of transition from  $\tilde{s}$  to  $\tilde{s}'$  by executing a. In order to optimize  $\eta$ , the reward function is defined as the single-transmission efficiency, namely

$$R(\tilde{\mathbf{s}}, a, \tilde{\mathbf{s}}') = \mathbf{1}(s_D' = 0)\mathbf{1}(a = i)L_P/L_i$$
 (19)

for i = 0, 1, 2.

Let  $q_m(\mathbf{s})$  be the joint belief regarding the decompressor and the channel's state  $\mathbf{s}$  at time m. Denote the  $|\mathcal{S}|$ -by-1 vector  $\mathbf{q}_m$  whose entries are  $q_m(\mathbf{s})$ ,  $\mathbf{s} \in \mathcal{S}$  as the belief vector of the POMDP system at m, which is updated by the observation  $\mathbf{o}$  and the action a via [50, eqs. (12.2) and (12.3)]. The goal of our POMDP formulated from the ROHC design problem is to find an optimal policy  $\pi$ , which maps belief of the state at m to an action, namely  $a_m = \pi(\mathbf{q}_m)$ , to maximize the infinite-horizon discounted reward:

$$\max_{\pi} \sum_{n=0}^{+\infty} \gamma^{n} \cdot \mathbb{E}\left[R(\mathbf{s}_{n}, \pi(\mathbf{q}_{n}), \mathbf{s}_{n+1})\right], \tag{20}$$

with discount factor  $0 < \gamma < 1$ .

Due to the choice of the reward function in Eq. (19), our POMDP maximizes the discounted sum of instantaneous transmission efficiency instead of the asymptotic efficiency

$$\mathbb{E}\left[\frac{\sum_{n=0}^{\infty} L_p \mathbf{1}(s_D[n]=0)}{\sum_{n=0}^{\infty} L_{s_C[n]}}\right] \to \sum_{n=0}^{\infty} \gamma^n \mathbb{E}\left[\frac{L_p \mathbf{1}(s_D[n]=0)}{L_{s_C[n]}}\right] \quad (21)$$

to formulate a classical POMDP, where  $s_C[n]$ ,  $s_D[n]$  denote the state of the compressor and the decompressor at time n, respectively and  $\mathbf{1}(\cdot)$  denotes the indicator function.

The solution to the POMDP problem termed policy is a set of "lower bound planes" vectors  $\mathcal{V} = \{\alpha\}$  of dimension  $|\tilde{\mathcal{S}}|$  [51]. Each vector is associated with an action  $a[\alpha] \in \mathcal{A}$ . The optimal action is selected with a simple online look-up according to the belief vector  $\mathbf{q}$ :

$$\hat{a}(\mathbf{q}) = a \left[ \arg \max_{\alpha \in \mathcal{V}} \alpha^T \mathbf{q} \right]. \tag{22}$$

Now we have established the basic POMDP model for the optimal control of ROHC when lower layer information is available with zero delay. To address practical issues, in the next section we will generalize the POMDP framework by considering delayed lower layer information.

#### C. POMDP Given Observation Signal Delay

For practical systems, we must take into account the effect of observation delay d. One classic approach is to augment the state space with the action history such that  $\tilde{s}_d = (\mathbf{a}_d, s_{D,d}, s_{H,d}) \in \tilde{S}_d = \mathcal{A}^d \times \tilde{S}$ , where  $\mathbf{a}_d = [a_1, \dots, a_d]$  to incorporate  $a_i$  as the action taken i-ROHC packets ago. Note that  $s_{D,d}$  and  $s_{H,d}$  are, respectively, the decompressor's state and the channel's state going back d ROHC packets in time. As a result, the dimension of the state space grows from  $\dim(\tilde{S}) = (W+3)K$  to  $\dim(\tilde{S}_d) = 3^d(W+3)K$ . Furthermore, the observation obtained with delay is represented as  $\mathbf{o}_d = (o_{T,d}, o_{H,d}) \in \Omega$ .

The POMDP formulation under observation delay of d packets are then augmented as follows. The probability transition function  $T_d(\tilde{\mathbf{s}}_d, a, \tilde{\mathbf{s}}_d')$  is redefined as:

$$T_d(\tilde{\mathbf{s}}_d, a, \tilde{\mathbf{s}}_d') = p(s_{H,d}'|s_{H,d}) p(s_{D,d}'|s_{D,d}, a_d, s_{H,d}') \times \delta(\mathbf{a}_d, a, \mathbf{a}_d')$$
(23)

where

$$\delta(\mathbf{a}_d, a, \mathbf{a}'_d) = \mathbf{1}(a'_1 = a) \prod_{i=2}^d \mathbf{1}(a'_i = a_{i-1})$$
 (24)

The observation function  $O(\tilde{\mathbf{s}}'_d, a, \mathbf{o}_d) : \tilde{\mathcal{S}}_d \times \mathcal{A} \times \Omega \to [0, 1]$ 

$$O(\tilde{\mathbf{s}}'_d, a, \mathbf{o}_d) = p(o_{H,d}|s'_{H,d})p(o_{T,d}|s'_{D,d}, a_d, s'_{H,d}).$$
 (25)

And the reward function  $R(\tilde{\mathbf{s}}_d, a, \tilde{\mathbf{s}}'_d) : \tilde{\mathcal{S}}_d \times \mathcal{A} \times \tilde{\mathcal{S}}_d \to \mathbb{R}$ 

$$R(\tilde{\mathbf{s}}_d, a, \tilde{\mathbf{s}}_d') = \frac{L_P}{L_{a_d}} \delta(\mathbf{a}_d, a, \mathbf{a}_d') \mathbf{1}(s_{D,d}' = 0). \tag{26}$$

We shall present a general POMDP solution and a detailed complexity analysis in Section V.

# V. SOLVING THE POMDP DESIGN PROBLEM AND COMPLEXITY ANALYSIS

It is generally intractable to solve POMDP problems exactly due to its prohibitive complexity [52], [53]. Nevertheless, there are efficient approximated POMDP solving techniques such as MDP-based heuristics and point-based value iteration methods (See references in [50, Sec. 12.3]) and many implementations [54]–[58]. In this work, we adopt the SARSOP algorithm [54], [59] to solve the POMDP problems on a general-purpose PC (with an Intel Core-i7 4790 CPU and 16GB DDR3 memory), which can provide decent solutions for state space with dimension of  $\sim 10^4$  within a few seconds. Since the POMDP needs only to be solved **once** for given system settings, our proposed algorithm can be executed during each the ROHC negotiation process or even offline followed by a policy look-up. Hence, algorithm of such complexity level is in fact practical.

The online complexity for our trans-layer ROHC compressor to determine the header type for each packet transmitted originates from two operations. First, for the belief update, the main computational overheads are in the evaluation of the *a priori* belief on state  $\tilde{\mathbf{s}}'_d$  caused by an action *a* without observation [50, eqs. (12.2) and (12.3)], namely

$$q_a(\tilde{\mathbf{s}}_d') = \sum_{\tilde{\mathbf{s}}_d \in \tilde{\mathcal{S}}_d} p(\tilde{\mathbf{s}}_d' | \tilde{\mathbf{s}}_d, a) q(\tilde{\mathbf{s}}_d)$$
 (27)

WLSB	W = 5
Header/Payload	$L_0 = 59, L_1 = 15, L_2 = 1, L_P = 20$
Channel	$l_B = 5, \epsilon = 0.1; \rho_B = 0.1, \rho_G = 0.9$
Markov Comp.	$n_{max} = 20$
POMDP Comp.	$d = 2, \lambda = 10^4; P_{FA} = P_{MD} = 0.1$ $P(o_H = B s_H' = G) = P(o_H = G s_H' = B) = 0.1$

TABLE I
THE DEFAULT SIMULATION SETTINGS

which can be evaluated as a matrix-vector product  $\mathbf{q}_a = \mathbf{T}_{a,d}\mathbf{q}$ , where  $\mathbf{q}_a$ ,  $\mathbf{q}$ ,  $\mathbf{T}_{a.d}$  represent the belief vectors corresponding to  $q_a(\tilde{s}_d'), q(\tilde{s}_d)$  and the transition probabilities  $p(\tilde{s}_d'|\tilde{s}_d, a)$ , respectively, for  $\tilde{s}_d', \tilde{s}_d \in \tilde{\mathcal{S}}_d$ . Due to the sparsity of the transition matrix  $\mathbf{T}_{a,d}$ , for each given action a, the complexity to compute all  $q_a(\tilde{s}_d')$  is  $O(|\tilde{\mathcal{S}}_d|K)$ .

Second, the optimal action selection in (22) requires the evaluation of  $\mathbf{Aq}$ , where  $\mathbf{A}$  is a  $|\mathcal{V}|$ -by- $|\tilde{\mathcal{S}}_d|$  matrix whose rows correspond to  $\alpha \in \mathcal{V}$ . In practice  $|\mathcal{V}|$  is usually of the same order of scale as  $|\tilde{\mathcal{S}}_d|$ . An effective approach to lower this complexity is to replace the policy matrix  $\mathbf{A}$  with its l-rank approximation  $\mathbf{A}_l = \mathbf{U}_{:,1:l} \boldsymbol{\Sigma}_{1:l,1:l} (\mathbf{V}_{:,1:l})^T$  where  $\mathbf{A} = \mathbf{U} \boldsymbol{\Sigma} \mathbf{V}^T$  is the SVD of  $\mathbf{A}$  [60]. Since the SVD only needs to be performed once, it does not account for the online complexity.

Let  $\mathcal{R}$  be the set of rows of matrix  $\mathbf{U}_{:,1:\ell} \Sigma_{1:\ell,1:\ell}$  and  $a[\mathbf{r}] \in \mathcal{A}$  be the action associated with the same row in  $\mathbf{A}$  as  $\mathbf{r}$  in  $\mathbf{A}_l$ . The policy-lookup in (22) can be evaluated in two steps:

$$\mathbf{b}_V = (\mathbf{V}_{:,1:\ell})^T \mathbf{b}$$
, and  $\hat{a}(\mathbf{b}) = a \left[ \arg \max_{\mathbf{r} \in \mathcal{R}} \mathbf{r}^T \mathbf{b}_V \right]$ , (28)

Consequently, the reduced complexity for policy look-up becomes  $O(|\tilde{S}_d|\ell + |\mathcal{V}|\ell)$ . In our test  $\ell$  is determined by parameter  $\lambda$  such that  $\sigma_1/\sigma_\ell \leq \lambda$  and  $\sigma_1/\sigma_{\ell+1} > \lambda$ , where  $\sigma_i$  denotes the *i*-th largest singular value of **A**.

#### VI. NUMERICAL EXAMPLES AND RESULTS

In this section, we present examples and numerical results to demonstrate the efficient design of the Markov compressor and the POMDP compressor, and compare their performances under various settings and measurements.

#### A. Test Setup

Unless otherwise noted, we consider a ROHC system with the settings as listed in Table. I. Here the WLSB window width is set to 3 according to [23] for higher packet loss rate, which corresponds to W = 5. Larger W results in stronger robustness to lossy channels at the expense of larger compressed header size and/or fewer CRC bits in the compressed headers. We consider a typical IPv6/UDP/RTP stream. Different header types have the following different structures [4, Sec. 5.7]:

- IR packet: packet type (1 octet) + profile (1 octet) + CRC (1 octet) + IPv6 (38 octets) + UDP (6 octets) + RTP (12 octets) = 59 octets.
- FO packet (IR-DYN): packet type (1 octet) + profile (1 octet) + CRC (1 octet) + IPv6-dyn (2 octets) + UDP-dyn (2 octets) + RTP-dyn (8 octets) = 15 octets.
- SO packet (UO-0): 1 octet.

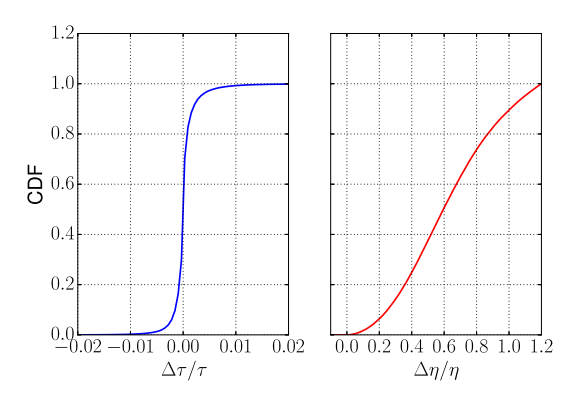


Fig. 7. Cumulative density of the relative error of  $\tau$  and  $\eta$  from the surrogate Markov compressor. Here  $\Delta \tau = \tau(\bar{\mathbf{P}}_C) - \tau(\mathbf{P}_C)$  and  $\Delta \eta = \eta(\bar{\mathbf{P}}_C) - \eta(\mathbf{P}_C)$ .

The length of a typical VoIP payload can be as low as 20 bytes [61]. The channel model considered in our simulation is the Gilbert-Elliot model defined with the average duration of a sequence of "bad" states  $l_B$ , or mean error burst length, and the steady-state probability of the "bad" state  $\epsilon$ , which are set to some realistic values as in [21] and [43] and mapped to state transition probability with  $p(s'_H = G|s_H = B) = 1/l_B$ ,  $p(s'_H = B|s_H = G) = p(s'_H = G|s_H = B)/(1/\epsilon - 1)$ . The successful transmission probability  $\rho_G$  and  $\rho_B$  are selected to characterize that the "good" and "bad" state may not be so clearly-cut. For the POMDP compressor, we assume a default channel state estimation error probability of 0.1. All the POMDP instances in this section are solved within 30 seconds with the maximum gap between the upper and lower bound of the value function returned by SARSOP to be 4.78%.

# B. Optimization of U-Mode Compressor With Markov Approximation

In Fig. 7 we firstly verify the fact that  $\tau(\mathbf{P}_C) \approx \tau(\bar{\mathbf{P}}_C)$  and that  $\eta(\bar{\mathbf{P}}_C) \gtrsim \eta(\mathbf{P}_C)$ . For this figure, 200000 instances of  $\mathbf{P}_C$  are generated randomly in which  $(P_{C,00}, P_{C,20})$ ,  $(P_{C,01}, P_{C,11}, P_{C,21})$  and  $(P_{C,02}, P_{C,12}, P_{C,22})$  are uniformly distributed on the 2-D/3-D simplex and the cumulative frequency histogram of the relative error of  $\eta(\bar{\mathbf{P}}_C)$  and  $\tau(\bar{\mathbf{P}}_C)$  w.r.t  $\eta(\mathbf{P}_C)$  and  $\tau(\mathbf{P}_C)$ , respectively, are evaluated numerically. As expected,  $\bar{\mathbf{P}}_C$  in general achieves approximately the same or better performances as compared with  $\mathbf{P}_C$ , thereby justifying the use of  $\hat{P}_{C,01} = \hat{P}_{C,02} = 0$ .

Fig. 8 demonstrates the optimization of  $d_1$ ,  $d_2$  of a timerbased ROHC compressor by mapping them into  $P_{C,11}$  and  $P_{C,22}$  and optimizing the latter accordingly. The empirical performance of the timer-based compressor is shown in filled contour graph. The optimal solution (marked with "o") for our default settings is  $\hat{P}_{C,11} = 0.000$  and  $\hat{P}_{C,22} = 0.895$ , corresponding to  $d_1 = 1$  and  $d_2 \approx 10$ . We find that  $\hat{P}_{C,11} = 0$  is generally true for better channel settings asymptotically, which is consistent with [19]. Also,  $\eta$  drops sharply when  $P_{C,22}$  approaches 1, i.e. when the FO packets are not transmitted frequently enough to maintain context synchronization. On the other hand, it appears that  $\eta$  is less sensitive to smaller  $P_{C,22}$ , implying that conservative strategy of transmitting more

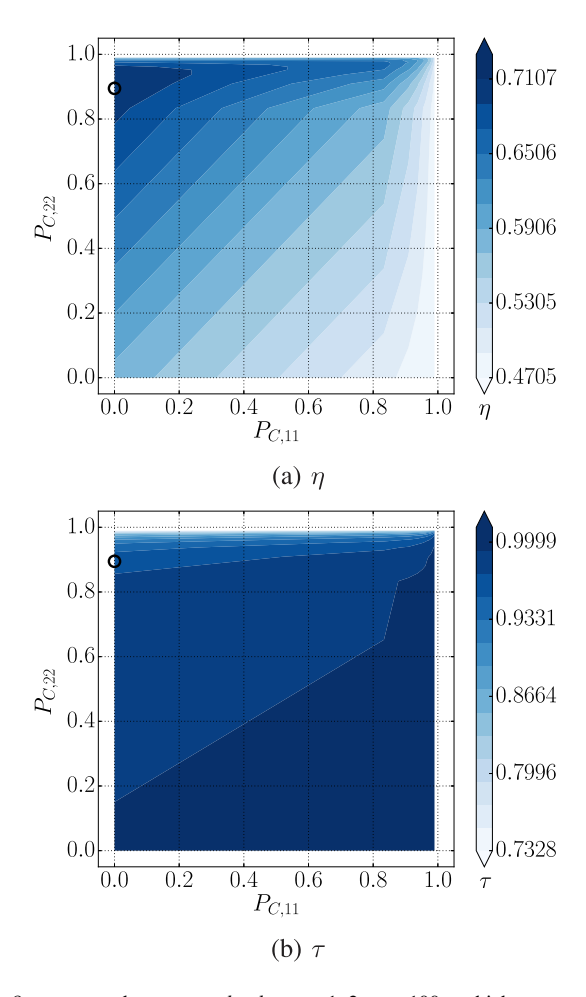


Fig. 8.  $\eta$  and  $\tau$  over  $d_1,d_2=1,2,\ldots,100$ , which are mapped to  $P_{C,11}=1-1/d_1$  and  $P_{C,22}=1-1/d_2$  and plotted with 2-D filled contour graphs. The optimized transition probability  $\hat{P}_{C,11}$  and  $\hat{P}_{C,22}$  are marked with a "o". The gap between the optimal performance from the Markov compressor and the timer-based compressor is 1.89%.

FO packets is better than the aggressive strategy of sending fewer FO packets, especially under inaccurate channel estimates. We also notice that max  $\eta$  corresponds to a compression transparency of  $\tau=0.95$ , suggesting that the efficiency is maximized at the cost of minor loss in the transparency.

#### C. Demonstration of POMDP Belief Update

In Fig. 9, we demonstrate the mechanism of how our POMDP compressor observes and estimates the channel and transmission status, updates its belief on the state of the ROHC system, and determine the type of packets to transmit. For simplicity we consider d=0. Some interpretation about this result are as follows:

- At n = 0, the belief on the channel follows its stationary distribution and the decompressor state is NC, therefore an IR packet is transmitted.
- At n=1, the POMDP compressor observes that the last channel state was "good" and the transmission was successful. Reflected by the updated belief, the decompressor is likely in FC<sub>0</sub> state. Consequently, a SO packet is transmitted.

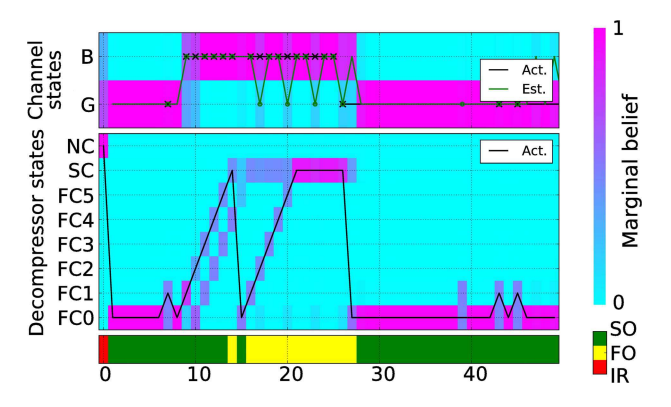


Fig. 9. Evolution of the marginal belief of the POMDP compressor on the channel and the decompressor's state versus the actual (Act.) states. The estimated (Est.) channel and transmission states are also plotted. Transmission failures are represented with markers.

- At n = 6, the last channel observation was "bad" and the last transmission observation was a failure; Thus there is a moderate possibility that the decompressor is in FC<sub>1</sub>.
- At n = 10, the last channel observation was "bad" but the last transmission observation was a success. However, these two estimations seem contradictory since a bad channel rarely results in a successful transmission. Consequently, in the belief update we observe a "splitting" phenomenon with a moderate belief for the decompressor in both FC<sub>0</sub> and FC<sub>2</sub> states. This phenomenon is also observed in n = 7, n = 27 and n = 28.
- Starting from n = 9, there are 6 consecutive transmission failures. At n = 14, the belief for the decompressor in SC state is already high. As a result, the compressor begins to transmit FO packet. At n = 15, due to the "splitting" phenomenon, the decompressor is most likely to have reverted to FC<sub>0</sub> state; Hence a SO packet is transmitted.
- At n = 16, we observe a "merging" phenomenon. Due to the "splitting" at n = 10, the belief on the decompressor's state at n = 15 focuses mainly on FC<sub>5</sub> and SC, apart from FC<sub>0</sub>. Then an observation of failed transmission suggests transitioning into SC from both FC<sub>5</sub> and SC, i.e. the two beliefs combine into a single larger belief on SC. As a result, the compressor decides to transmit a FO packet. This phenomenon also manifests at n = 21.
- At n = 28, the observation of a successful transmission and "good" channel state gives the POMDP compressor a higher confidence that the decompressor is back in FC<sub>0</sub> state. Consequently, SO packets are transmitted for ensuing transmissions.

## D. Empirical Performance

In Fig. 10, we demonstrate the evolution of the empirical efficiency  $\eta[n]$ , i.e. the average of the ratio between the total successfully decompressed bits over the total transmitted bits (cumulative). We compare the empirical performance of the conventional timer-based compressor optimized with the Markov approximation technique in Sec. III (red lines) and that of the POMDP compressor (the blue line). For reference purpose, we also plot (black lines) the expected efficiency

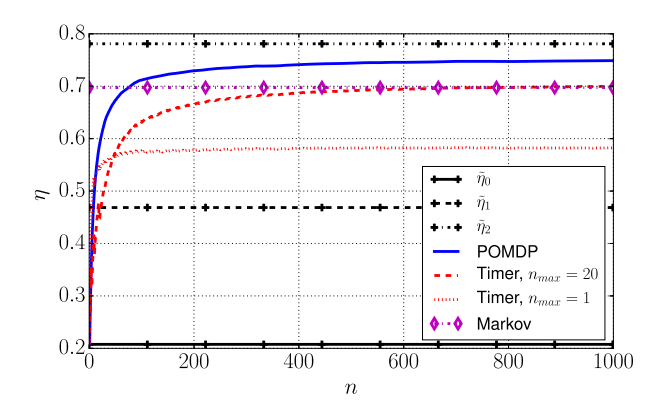


Fig. 10. Evolution of the empirical efficiency  $\eta$ .

when a single type of header is used assuming no OoS, namely

$$\tilde{\eta}_a = \rho_a^T \pi_H \frac{L_p}{L_a}, \quad a = 0, 1, 2$$
 (29)

where  $\pi_H$  is the stationary distribution of the Markov channel. Apparently  $\tilde{\eta}_2$  is an upper-bound of transmission efficiency for all tested ROHC schemes. We also plot the theoretical efficiency maximized with the Markov approximation in (14) (the magenta line). To demonstrate the necessity of the slow-start phase, we also plotted the performance of the timer-based Markov compressor with  $n_{max} = 1$ , i.e. only 1 IR packet is transmitted to establish context synchronization.

It is important to note that the performance gain of the POMDP compressor over the optimized timer-based compressor is two-fold. First, the asymptotic efficiency of the former surpasses the latter by about 10%. Second, the efficiency of the POMDP compressor grows much faster than that of the timer-based compressor. In fact, the performance gain of the POMDP compressor over the Markov compressor is over 15% for  $n \le 80$ . This suggests that the POMDP compressor outperforms the conventional U-mode compressor by an even larger margin when the packet stream requires frequent context re-initialization. Hence, our proposed POMDP compressor for ROHC exhibits much better applicability than the conventional U-mode ROHC compressor.

In Fig. 11, we demonstrate the performance gain of the POMDP compressor over the Markov compressor when inaccurate trans-layer information is available. We let  $P_{\text{FA}} = P_{\text{MD}} = P_{e,T}$  and  $p(o_H = B|s'_H = G) = p(o_H = G|s'_H = B) = P_{e,H}$ , which define the accuracy of the transmission status the channel state estimation, respectively. As our results show, the performance is more sensitive to the former accuracy. Nevertheless, when at least one of the two estimators exhibits a moderate accuracy, the POMDP compressor achieves a substantial performance gain over the timer-based compressor.

We also notice that there are two special cases herein. On one hand, the case of  $P_{e,T}=0$  and  $P_{e,H}=0.5$  is equivalent to a conventional R-mode compressor, where each packet transmission results in an ACK/NACK, with the same feedback delay. The performance of the POMDP compressor can approach that of the R-mode compressor even under moderate

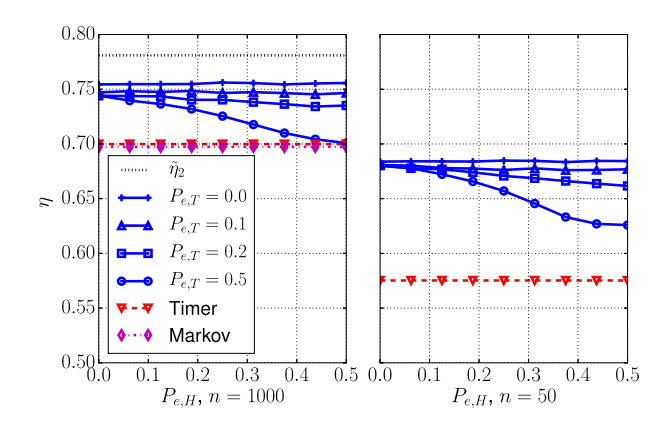


Fig. 11. Empirical efficiency  $\eta$  of the POMDP compressor versus estimator accuracy for POMDP compressor (blue), timer-based compressor (red) and the theoretical value given by the Markov approximation technique (magenta).

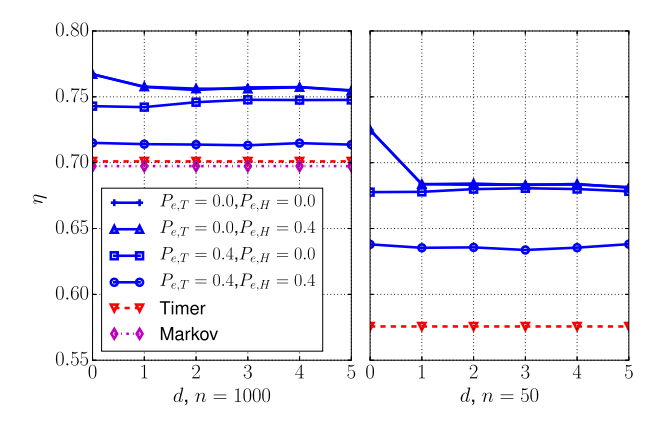


Fig. 12. Empirical efficiency  $\eta$  versus estimator delay.

estimation error. On the other hand, the case of  $P_{e,T} = 0.5$  and  $P_{e,H} = 0.5$  is equivalent to a U-mode compressor whose actions fully rely on the underlying unobservable Markov decision process (UOMDP). As we can see, its asymptotic performance is close to that of the Markov compressor, which justifies our Markov approximation technique for efficiency optimization.

The impact of the observation delay d on the POMDP compressor is demonstrated in Fig. 12. The results show that a transmission/channel state estimation delay d up to 5 packets has little impact. However, when only a small number of packets are transmitted, the effect of an observation with non-zero delay on the performance can be more noticeable.

Next we test the performance against various channel conditions. In Fig. 13 and Fig. 14, we demonstrate the performance of the POMDP and the Markov compressor under different channel quality ( $\epsilon$ ) and time-correlation ( $l_B$ ) settings, respectively. Apparently, the POMDP compressor is more robust against poor channel conditions. Intuitively, when the channel is nearly perfect ( $\epsilon \rightarrow 0$ ) or when the Markov channel degenerated into a time-independent and random channel (labeled as  $l_B = 0$ ), the gain on asymptotic efficiency of the POMDP compressor over the optimized timer-based compressor diminishes. In fact, in comparison with the upper-

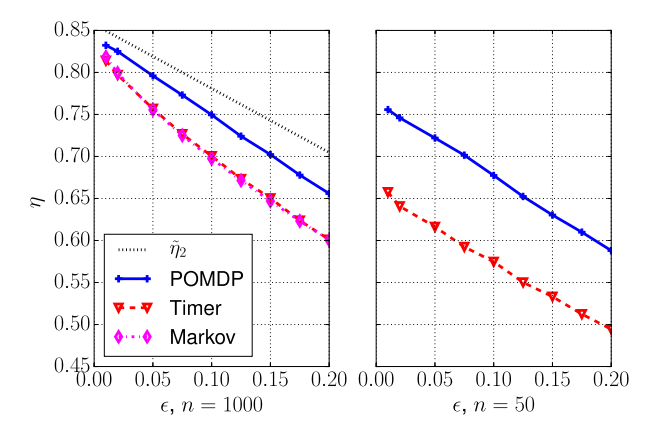


Fig. 13. Empirical efficiency  $\eta$  versus the stationary probability of "bad" state  $\epsilon$ .

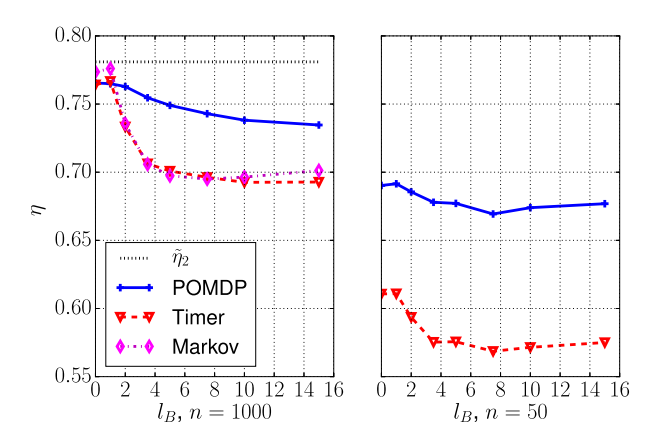


Fig. 14. Empirical efficiency  $\eta$  versus the expected length of consecutive "bad" states  $l_B$ .

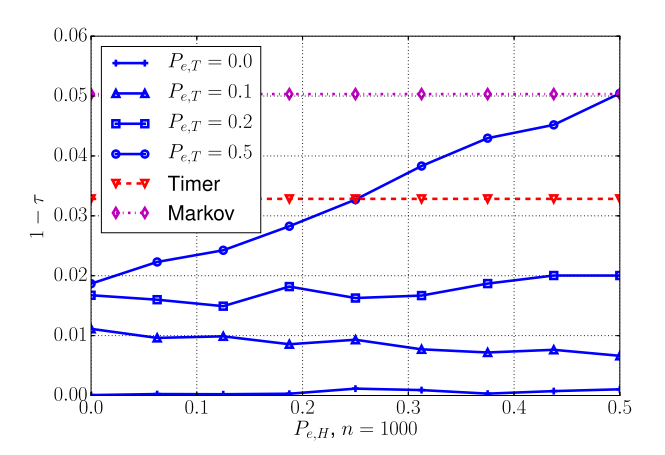


Fig. 15. Compression transparency  $\tau$  versus estimator accuracy.

bound  $\tilde{\eta}_2$ , we note that there is little room for improvement as the optimized U-mode compressor already performs well. Even in this case, the POMDP remains advantageous when only a small number of packets are transmitted before re-initialization. On the other hand, when the channel is in poorer condition with larger  $\epsilon$  and longer coherence time, the POMDP compressor outperforms the timer-based compressor by a larger margin, both in stationary efficiency and short-term transient efficiency.

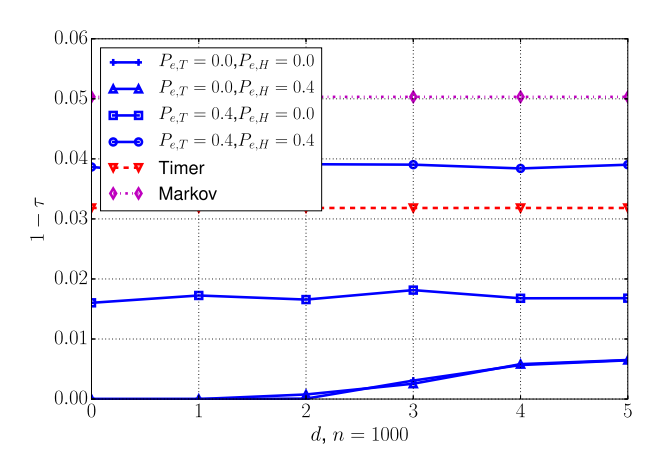


Fig. 16. Compression transparency  $\tau$  versus estimator delay.

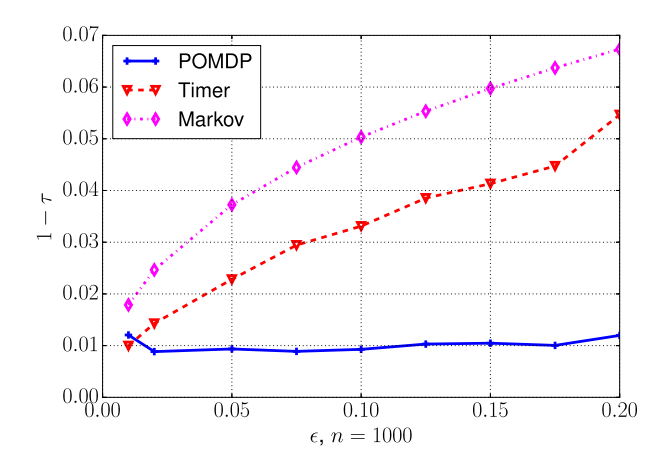


Fig. 17. Compression transparency  $\tau$  versus  $\epsilon$ .

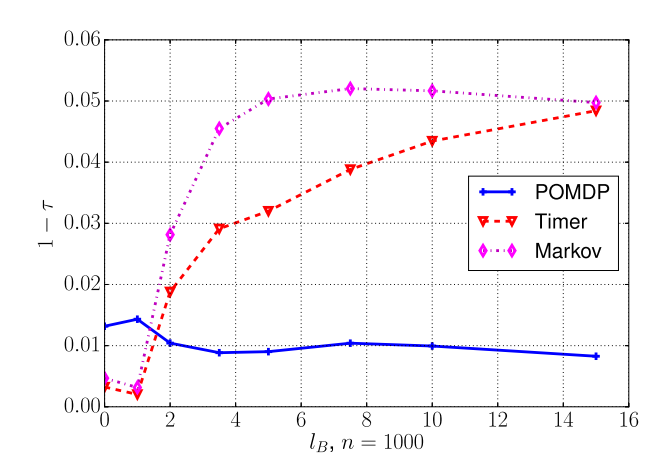


Fig. 18. Compression transparency  $\tau$  versus  $l_B$ .

As mentioned earlier, the conventional ROHC compressor cannot maintain high compression transparency and high transmission efficiency at the same time. In comparison, the POMDP compressor optimized for maximum transmission efficiency also outperforms the timer-based compressor in terms of compression transparency. In Fig. 15-Fig. 18, the empirical compression transparency  $\tau$  of the POMDP compressor is compared with that of the optimized timer-based compressor under the same estimation accuracy/delay and channel settings as in the previous simulations. We observe

a performance gain in compression transparency similar to that in transmission efficiency, as long as the quality of the translayer information is not too low.

#### VII. CONCLUSION

This work formulates and investigates the optimization and a trans-layer design of U-mode RObust Header Compression (ROHC) for improving payload efficiency in wireless packet networks. For networks using a traditional timer-based header compressor, we present an optimization scheme based on a Markov approximation technique, which enables efficient evaluation and optimization of various performance measurements. For networks exploiting trans-layer signaling to further boost the performance of ROHC, we propose a trans-layer compressor design which makes use of the information from lower layers regarding the channel state and the packet loss status. We propose a novel application of partially observable Markov decision process (POMDP) such that the new ROHC compressor can update its belief on the wireless channel and the decompressor states based on imperfect and delayed observations and adjust the compression level accordingly. Our numerical results show that the Markov compressor model can closely imitate a general timer-based compressor and can be effectively optimized. We demonstrate great potential for the trans-layer ROHC compressor based on POMDP to further improve the stationary packet efficiency and agility against frequent context re-initialization, under various channel settings and qualities of the trans-layer information.

#### REFERENCES

- D. Naidu and R. Tapadiya, "Implementation of header compression in 3GPP LTE," in *Proc. 6th Int. Conf. Inf. Technol., New Generat.*, Apr. 2009, pp. 570–574.
- [2] The Concept of Robust Header Compression, ROHC, Effnet AB, Luleå, Sweden, 2004.
- [3] E. Martinez, A. Minaburo, and L. Toutain, "Cross layer ROHC compression for multicast video streaming," in *Proc. IEEE Veh. Technol. Conf.*, May 2008, pp. 2878–2882.
- [4] C. Bormann et al., RObust Header Compression (ROHC): Framework and Four Profiles: RTP, UDP, ESP, and Uncompressed, document RFC 3095, Internet Engineering Task Force (IETF), Fremont, CA, USA, Mar. 2001.
- [5] G. Pelletier and K. Sandlund, RObust Header Compression Version 2 (ROHCv2): Profiles for RTP, UDP, IP, ESP and UDP-Lite, document RFC 5225, Internet Engineering Task Force (IETF), Fremont, CA, USA, Apr. 2008.
- [6] K. Sandlund, G. Pelletier, and L.-E. Jonsson, The RObust Header Compression (ROHC) Framework, document RFC 5795, Internet Engineering Task Force (IETF), Fremont, CA, USA, Mar. 2010.
- [7] Evolved Universal Terrestrial Radio Access (E-UTRA); Packet Data Convergence Protocol (PDCP) Specification, Technical Specification, 3GPP, document TS 36.323 (v13.2.1), 2016.
- [8] A. Al-Fuqaha, M. Guizani, M. Mohammadi, M. Aledhari, and M. Ayyash, "Internet of Things: A survey on enabling technologies, protocols, and applications," *IEEE Commun. Surveys Tuts.*, vol. 17, no. 4, pp. 2347–2376, 4th Quart., 2015.
- [9] C. Bormann, 6LoWPAN-GHC: Generic Header Compression for IPv6 Over Low-Power Wireless Personal Area Networks (6LoWPANs), RFC, document 7400, Nov. 2014.
- [10] Y. Niu, C. Wu, L. Wei, B. Liu, and J. Cai, "Backfill: An efficient header compression scheme for OpenFlow network with satellite links," in *Proc. Int. Conf. Netw. Netw. Appl.*, Jul. 2016, pp. 202–205.
- [11] B.-N. Cheng, J. Wheeler, and B. Hung, "Internet protocol header compression technology and its applicability on the tactical edge," *IEEE Commun. Mag.*, vol. 51, no. 10, pp. 58–65, Oct. 2013.

- [12] M. Tömösközi, P. Seeling, P. Ekler, and F. H. P. Fitzek, "Performance evaluation and implementation of IP and robust header compression schemes for TCP and UDP traffic in the wireless context," in *Proc.* 4th Eastern Eur. Reg. Conf. Eng. Comput. Based Syst., Aug. 2015, pp. 45–50.
- [13] B. Hung, D. Defrancesco, B.-N. Cheng, and P. Sukumar, "An evaluation of IP header compression on the GIG joint IP modem system," in *Proc. IEEE Military Commun. Conf.*, Oct. 2014, pp. 1484–1490.
- [14] A. Maeder and A. Felber, "Performance evaluation of ROHC reliable and optimistic mode for voice over LTE," in *Proc. IEEE 77th Veh. Technol. Conf.*, Jun. 2013, pp. 1–5.
- [15] M. Tömösközi, P. Seeling, and F. H. P. Fitzek, "Performance evaluation and comparison of RObust Header Compression (ROHC) ROHCv1 and ROHCv2 for multimedia delivery," in *Proc. IEEE Globecom Workshops*, Dec. 2013, pp. 544–549.
- [16] T. Tordjman and O. Lücke, "Evaluation of robust header compression for aeronautical operational data," in *Proc. 12th Signal Process. Space Commun. Workshop*, Sep. 2012, pp. 308–315.
- [17] E. Piri, J. Pinola, F. Fitzek, and K. Pentikousis, "ROHC and aggregated VoIP over fixed WiMAX: An empirical evaluation," in *Proc. IEEE Symp. Comput. Commun.*, Jul. 2008, pp. 1141–1146.
- [18] F. H. P. Fitzek, S. Rein, P. Seeling, and M. Reisslein, "RObust header compression (ROHC) performance for multimedia transmission over 3G/4G wireless networks," Wireless Pers. Commun., vol. 32, no. 1, pp. 23–41, 2005.
- [19] A. Minaburo, L. Nuaymi, K. D. Singh, and L. Toutain, "Configuration and analysis of robust header compression in UMTS," in *Proc. IEEE 14th Pers.*, *Indoor Mobile Radio Commun.*, vol. 3. Sep. 2003, pp. 2402–2406.
- [20] B. Wang, H. P. Schwefel, K. C. Chua, R. Kutka, and C. Schmidt, "On implementation and improvement of robust header compression in UMTS," in *Proc. IEEE 13th Int. Symp. Pers., Indoor Mobile Radio Commun.*, vol. 3. Sep. 2002, pp. 1151–1155.
- [21] R. Hermenier, F. Rossetto, and M. Berioli, "On the behavior of RObust header compression U-mode in channels with memory," *IEEE Trans. Wireless Commun.*, vol. 12, no. 8, pp. 3722–3732, Aug. 2013.
- [22] R. Hermenier, F. Rossetto, and M. Berioli, "A simple analytical model for robust header compression in correlated wireless links," in *Proc. Int. Symp. Wireless Commun. Syst.*, Nov. 2011, pp. 634–638.
- [23] S. Kalyanasundaram, V. Ramachandran, and L. M. Collins, "Performance analysis and optimization of the window-based least significant bits encoding technique of ROHC," in *Proc. IEEE Global Telecommun. Conf.*, Nov. 2007, pp. 4681–4686.
- [24] C. Y. Cho, W. K. G. Seah, and Y. H. Chew, "A framework and source model for design and evaluation of robust header compression," *Comput. Netw.*, vol. 50, no. 15, pp. 2676–2712, Oct. 2006.
- [25] H. Wang and K. G. Seah, "An analytical model for the ROHC RTP profile," in *Proc. IEEE Wireless Commun. Netw. Conf.*, vol. 1. Mar. 2004, pp. 126–131.
- [26] A. Couvreur, L.-M. L. Ny, A. Minaburo, G. Rubino, B. Sericola, and L. Toutain, "Performance analysis of a header compression protocol: The ROHC unidirectional mode," *Telecommun. Syst.*, vol. 31, no. 1, pp. 85–98, 2006.
- [27] M. Degermark, B. Nordgren, and S. Pink, "IP header compression, RFC 2507," Tech. Rep., Feb. 1999.
- [28] P. Barber, "Cross layer design for ROHC and HARQ," IEEE 802.16 Broadband Wireless Access Working Group, Tech. Rep. IEEE C802.16 m-09/2559r1, 2009.
- [29] A. R. Cassandra, "A survey of POMDP applications," in Proc. Working Notes AAAI Fall Symp. Planning Partially Observable Markov Decision Processes, 1998, pp. 17–24.
- [30] G. E. Monahan, "State of the art—A survey of partially observable Markov decision processes: Theory, models, and algorithms," *Manage. Sci.*, vol. 28, no. 1, pp. 1–16, 1982.
- [31] M. Hirzallah, W. Afifi, and M. Krunz, "Full-duplex-based rate/mode adaptation strategies for Wi-Fi/LTE-U coexistence: A POMDP approach," *IEEE J. Sel. Areas Commun.*, vol. 35, no. 1, pp. 20–29, Jan. 2017.
- [32] J. Seo, Y. Sung, G. Lee, and D. Kim, "Training beam sequence design for millimeter-wave MIMO systems: A POMDP framework," *IEEE Trans. Signal Process.*, vol. 64, no. 5, pp. 1228–1242, Mar. 2016.
- [33] P. Rana, K. H. Li, and K. C. Teh, "Dynamic cooperative sensing—Access policy for energy-harvesting cognitive radio systems," *IEEE Trans. Veh. Technol.*, vol. 65, no. 12, pp. 10137–10141, Dec. 2016.

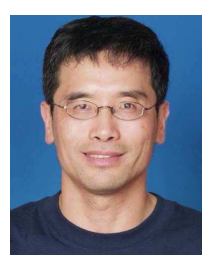
- [34] J. Wang, C. Jiang, Z. Han, Y. Ren, and L. Hanzo, "Network association strategies for an energy harvesting aided Super-WiFi network relying on measured solar activity," *IEEE J. Sel. Areas Commun.*, vol. 34, no. 12, pp. 3785–3797, Dec. 2016.
- [35] P. Si, Y. He, H. Yao, R. Yang, and Y. Zhang, "DaVe: Offloading delay-tolerant data traffic to connected vehicle networks," *IEEE Trans. Veh. Technol.*, vol. 65, no. 6, pp. 3941–3953, Jun. 2016.
- [36] M. Abu Alsheikh, D. T. Hoang, D. Niyato, H.-P. Tan, and S. Lin, "Markov decision processes with applications in wireless sensor networks: A survey," *IEEE Commun. Surveys Tuts.*, vol. 17, no. 3, pp. 1239–1267, Apr. 2015.
- [37] A. Fanous, Y. E. Sagduyu, and A. Ephremides, "Reliable spectrum sensing and opportunistic access in network-coded communications," *IEEE J. Sel. Topics Signal Process.*, vol. 32, no. 3, pp. 400–410, Mar. 2014.
- [38] A. Aprem, C. R. Murthy, and N. B. Mehta, "Transmit power control policies for energy harvesting sensors with retransmissions," *IEEE J. Sel. Topics Signal Process.*, vol. 7, no. 5, pp. 895–906, Oct. 2013.
- [39] Y. Li, S. K. Jayaweera, M. Bkassiny, and K. A. Avery, "Optimal myopic sensing and dynamic spectrum access in cognitive radio networks with low-complexity implementations," *IEEE Trans. Wireless Commun.*, vol. 11, no. 7, pp. 2412–2423, Jul. 2012.
- [40] Q. Zhao and J. Ye, "Quickest detection in multiple On–Off processes," IEEE Trans. Signal Process., vol. 58, no. 12, pp. 5994–6006, Dec. 2010.
- [41] R. Fracchia, C. Gomez, and A. Tripodi, "R-RoHC: A single adaptive solution for header compression," in *Proc. IEEE 73rd Veh. Technol. Conf.*, May 2011, pp. 1–5.
- [42] V. Suryavanshi and A. Nosratinia, "Error-resilient packet header compression," *IEEE Trans. Commun.*, vol. 56, no. 11, pp. 1836–1843, Nov. 2008.
- [43] L. Badia, N. Baldo, M. Levorato, and M. Zorzi, "A Markov framework for error control techniques based on selective retransmission in video transmission over wireless channels," *IEEE J. Sel. Areas Commun.*, vol. 28, no. 3, pp. 488–500, Apr. 2010.
- [44] E. O. Elliott, "Estimates of error rates for codes on burst-noise channels," Bell Syst. Tech. J., vol. 42, no. 5, pp. 1977–1997, Sep. 1963.
- [45] H. S. Wang and N. Moayeri, "Finite-state Markov channel-a useful model for radio communication channels," *IEEE Trans. Veh. Technol.*, vol. 44, no. 1, pp. 163–171, Feb. 1995.
- [46] P. Sadeghi, R. A. Kennedy, P. B. Rapajic, and R. Shams, "Finite-state Markov modeling of fading channels—A survey of principles and applications," *IEEE Signal Process. Mag.*, vol. 25, no. 5, pp. 57–80, Sep. 2008.
- [47] S. Sivaprakasam and K. S. Shanmugan, "An equivalent Markov model for burst errors in digital channels," *IEEE Trans. Commun.*, vol. 43, no. 2/3/4, pp. 1347–1355, Feb. 1995.
- [48] C. M. Bishop, Pattern Recognition and Machine Learning. New York, NY, USA: Springer, 2006
- [49] B. Mitavskiy, J. E. Rowe, A. Wright, and L. M. Schmitt, "Quotients of Markov chains and asymptotic properties of the stationary distribution of the Markov chain associated to an evolutionary algorithm," *Genetic Programm. Evol. Mach.*, vol. 9, no. 2, pp. 109–123, 2008.
- [50] M. T. Spaan, "Partially observable Markov decision processes," in Reinforcement Learning. Berlin, Germany: Springer, 2012, pp. 387–414.
- [51] E. J. Sondik, "The optimal control of partially observable Markov processes over the infinite horizon: Discounted costs," *Ope. Res.*, vol. 26, no. 2, pp. 282–304, 1978.
- [52] C. H. Papadimitriou and J. N. Tsitsiklis, "The complexity of Markov decision processes," *Math. Oper. Res.*, vol. 12, no. 3, pp. 441–450, 1987.
- [53] W. S. Lee, N. Rong, and D. J. Hsu, "What makes some POMDP problems easy to approximate?" in Adv. Neural Inform. Process. Syst., 2007, pp. 689–696.
- [54] (Apr. 18, 2017). APPL: Approximate POMDP Planning Toolkit. [Online]. Available: http://bigbird.comp.nus.edu.sg/pmwiki/farm/appl/
- [55] A. R. Cassandra. POMDP-Solve, accessed on Apr. 18, 2017. [Online]. Available: http://www.pomdp.org/code/
- [56] H. Kurniawati, D. Klimenko, J. M. Song, K. Seiler, and V. Yadav. TAPIR: Toolkit for Approximating and Adapting POMDP Solutions in Real Time, accessed on Apr. 18, 2017. [Online]. Available: http:// robotics.itee.uq.edu.au/~hannakur/dokuwiki/doku.php?id=wiki:tapi%r

- [57] D. Silver and J. Veness. Monte-Carlo Planning in Large POMDPs, accessed on Apr. 18, 2017. [Online]. Available: http://www0.cs.ucl.ac.uk/staff/D.Silver/web/Applications.html
- [58] E. Patrick. (Apr. 18, 2017). POMDPy. [Online]. Available: http://pemami4911.github.io/POMDPy/
- [59] O. Brock, J. Trinkle, and F. Ramos, "SARSOP: Efficient point-based POMDP planning by approximating optimally reachable belief spaces," in *Robotics: Science and Systems*, vol. 4. Cambridge, MA, USA: MITPress, 2009, pp. 65–72.
- [60] C. Eckart and G. Young, "The approximation of one matrix by another of lower rank," *Psychometrika*, vol. 1, no. 3, pp. 211–218, Sep. 1936.
- [61] Cisco. (2006). Voice Over IP–Per Call Bandwidth Consumption. http://www.cisco.com/c/en/us/support/docs/voice/voice-quality/7934bwid%th-consume.html



Wenhao Wu (S'12) received the B.S. degree in electrical information science and technology from Tsinghua University, Beijing, China, in 2012. He is currently pursuing the Ph.D. degree in electrical and computer engineering with the Broadband Radio Access Technologies Laboratory, University of California at Davis, Davis, CA, USA. During his Ph.D. studies, he conducted cooperative research with the Missouri University of Science and Technology, Rolla, MO, USA. His research interests include communications and information theory with special

emphasis on multiple-input multiple-output systems, signal processing for wireless communications, and trans-layer designs.



Zhi Ding (S'88–M'90–SM'95–F'03) received the Ph.D. degree in electrical engineering from Cornell University in 1990. From 1990 to 2000, he was a faculty member with Auburn University and later, the University of Iowa. He has held visiting positions at Australian National University, The Hong Kong University of Science and Technology, the NASA Lewis Research Center, and the USAF Wright Laboratory. He has active collaboration with researchers from several countries, including Australia, China, Japan, Canada, Taiwan, South Korea, Singapore, and

Hong Kong. He is currently a Professor of engineering and entrepreneurship with the University of California at Davis.

He has co-authored the text book *Modern Digital and Analog Communication Systems*, 4th edition, (Oxford University Press, 2009). He has been serving on the technical program committees of several workshops and conferences. He was a member of the Technical Committee on Statistical Signal and Array Processing and a member of the Technical Committee on Signal Processing for Communications from 1994 to 2003. He served as a Steering Committee Member of the IEEE TRANSACTIONS ON WIRELESS COMMUNICATIONS from 2007 to 2009 and the Chair from 2009 to 2010. He received the 2012 IEEE Wireless Communication Recognition Award from the IEEE Communications Society. He was the Technical Program Chair of the 2006 IEEE Globecom. He was also an IEEE Distinguished Lecturer (Circuits and Systems Society from 2004 to 2006 and Communications Society from 2008 to 2009). He was an Associate Editor of the IEEE TRANSACTIONS ON SIGNAL PROCESSING from 1994 to 1997 and from 2001 to 2004, and an Associate Editor of the IEEE SIGNAL PROCESSING LETTERS from 2002 to 2005.